IOP Conf. Series: Materials Science and Engineering **279** (2017) 012028 doi:10.1088/1757-899X/279/1/012028

Present status of PIT round wires of 122-type iron-based superconductors

T Tamegai[1], T Suwa[1], S Pyon[1], H Kajitani[2], K Takano[2], N Koizumi[2], S Awaji[3] and K Watanabe[3]

[1]Department of Applied Physics, The University of Tokyo, 7-3-1 Hongo, Bunkyo-ku, Tokyo 113-8656, Japan
[2] Naka Fusion Institute, National Institutes for Quantum and Radiological Science and Technology **(**QST), 801-1 Mukoyama, Naka-shi, Ibaraki 311-0193, Japan
[3]High Field Laboratory for Superconducting Materials, Institute for Materials Research, Tohoku University, Sendai 980-8577, Japan

E-mail: tamegai@ap.t.u-tokyo.ac.jp

Abstract. Outstanding characteristics with high T_c and H_{c2} and small anisotropy in iron-based superconductors (IBSs) have triggered the development of superconducting wires and tapes using these novel superconductors. In this short article, developments and present status of round wires of 122-type IBSs are reviewed. By introducing hot-isostatic pressing (HIP) technique, J_c in round wires of 122-type IBSs has been improved significantly. Further improvements have been realized by refining the fabrication process of the core material and introducing partial texturing of the wire core. The largest transport J_c for round wires at 4.2 K at self-field and 100 kOe are 2.0×10^5 A/cm^2 and 3.8×10^4 A/cm^2, respectively. We also compare the J_c characteristics of wires and tapes processed by HIP.

1. Introduction

Iron-based superconductors (IBSs) have very promising characteristics for high-field applications with their reasonably high T_c, H_{c2}, and J_c, and small anisotropy [1,2]. Among various IBSs, 122-type compounds are most extensively studied due to the fact that stable single crystals with good characteristics can be easily obtained. J_c close to 1.0×10^6 A/cm^2 at low temperatures is realized in single crystals of 122-type IBSs [3,4] and further enhancement of J_c by irradiation has also been demonstrated [5-7]. In particular, (Ba,K)Fe_2As_2 single crystal has a large J_c, and it can be enhanced over 1×10^7 A/cm^2 (4.2 K, self-field) after irradiation [8-10]. Several techniques have been applied to fabricate superconducting wires and tapes of IBSs [1]. Among them, round wires fabricated using the powder-in-tube (PIT) method is the simplest ones and the first wires using 1111-type IBS was fabricated using this technique [11]. In addition, round wires produced by PIT technique is most suitable for winding high-field magnets. Up to now, using 122-type IBSs, (Ba,K)Fe_2As_2 and (Sr,K)Fe_2As_2 PIT round wires have been fabricated, and reasonably high in-field J_c has been reported [8, 12-19]. On the other hand, J_c characteristics in tapes are better than round wires, in particular, in pressed tapes. The practical level of J_c of 1×10^5 A/cm^2 has been achieved even at 100 kOe in pressed tapes [20,21]. This is due to the high degree of texturing and high density in the pressed tape.

There are three kinds of sites where we can modify physical properties of 122-type IBSs, namely

(Ba,*A*)Fe_2As_2 (*A*: Alkali earths), Ba(Fe,*M*)$_2As_2$ (*M*: transition metals), and $BaFe_2(As,P)_2$. Among these three kinds of materials, $BaFe_2(As,P)_2$ is least extensively studied. Although reasonably high-quality bulk polycrystalline materials are reported, their J_c characteristics are not well known [22]. Actually, when the PIT wires are fabricated using $BaFe_2(As,P)_2$, only a small value of J_c~1,000 A/cm^2 (4.2 K, self-field) is realized possibly due to the presence of minor ferromagnetic impurity phase Fe_2P. The situation is similar in the case of $Ba(Fe,Co)_2As_2$. The largest J_c reported for wires of $Ba(Fe,Co)_2As_2$ is ~ 1x10^4 A/cm^2 at 4.2 K and self-field [14,19,23].

In this short article, present status of J_c characteristics of PIT round wires of 122-type materials are reviewed focusing on (Ba,K)Fe_2As_2. We report the latest result of the highest J_c of 3.8x10^4 A/cm^2 at 4.2 K under 100 kOe in (Ba,K)Fe_2As_2 PIT wire. Characterizations of the PIT wires including magneto-optical imaging and X-ray analyses are reported. We also compare the J_c characteristics of wires and tapes, both processed under high pressure.

2. Experiments

All the superconducting wires of 122-type IBSs were fabricated using powder-in-tube (PIT) method. For the last couple of years, we have constantly improved the fabrication processes. Five kinds of PIT wires of $Ba_{0.6}K_{0.4}Fe_2As_2$ are reported in this article [15-18]. Typical characteristics of these wires are summarized in Table 1.

Table 1. Characteristics of round wires of $Ba_{0.6}K_{0.4}Fe_2As_2$, #1 [15], #2 [16], #3 [17], #4 [18], and new wire #5. "G" and "D" in the drawing method mean "groove-roller" and "dies", respectively.

Wires	Drawing method	Sintering *T* (C^o)	Sintering *P* (MPa)	Sintering time (h)	Diameter (mm)	J_c (4.2 K, sf) (A/cm^2)	J_c (4.2 K, 10 T) (A/cm^2)
#1	G	900	0.1	36	0.6	1.0x10^4	500
#2	G	600	120	4	1.2	3.8x10^4	3.0x10^3
#3	G	700	175	0.5	1.2	1.2x10^5	9.0x10^3
#4	G	700	175	4	1.2	1.8x10^5	2.0x10^4
#5	G/D	700	175	4	1.2	2.0x10^5	3.8x10^4

In the first generation PIT wire #1, starting raw materials were mixed in a glove box filled with Ar gas but with insufficient purity, and the mixing process was performed by hand using agate mortar [15]. After the introduction of glove box with a gas purification function and planetary ball milling machine for pulverizing raw materials for wire #2-#5, J_c was improved significantly. We also introduced hot-isostatic pressing (HIP) process after wire #2 [16]. In the HIP process, starting powders are first filled in a Ag tube with inner diameter of 3 mm, and then drawn down to a diameter of 1.2 mm. After this, the drawn wire was put in a 1/8" outer diameter Cu tube and drawn to a final diameter of ~1.2 mm. After the drawing process, both ends were sealed by using arc welding. Details of wire fabrication conditions for each wire are described in the corresponding reference, except for the #5. In the latest wire fabrication #5, wire-drawing dies were introduced to make the wires into more perfect round shape, which also helped to make the cross section of the core more circular. Unfortunately, however, we had to introduce groove-roller in the last stage of the wire drawing, since wires were often broken in the drawing process using dies when the diameter became small.

Phase purity of the wire was confirmed by using X-ray diffraction. Shielding characteristics and magnetic J_c were characterized by using a commercial SQUID magnetometer (MPMS-XL5, Quantum Design). Transport J_c was evaluated at IMR, Tohoku university by using 15 T superconducting magnet. Electrical contacts to the wire were made by soldering, and the wire was immersed in liquid He to minimize the effect of heating. Magneto-optical (MO) imaging of the wires was performed after cutting the wire to reveal the specific cross section of the wire core and polishing them using lapping films. Magnetic induction distribution was visualized by using a garnet film. MO imaging was performed using a continuous-flow type of cryostat (Microstat-HR, Oxford Instruments), and the

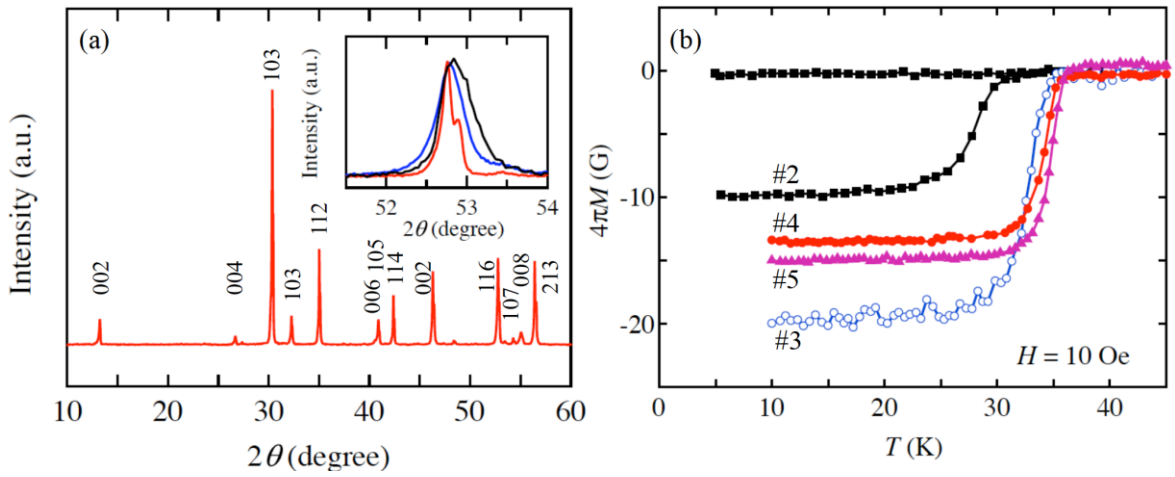

Figure 1. (a) X-ray diffraction pattern of (Ba,K)Fe_2As_2 powder for wire #4. Inset shows blow-ups of 116 peaks for wires #2 (black), #3 (blue), and #4 (red). (2) Magnetization as a function of temperature at 10 Oe for wires #2 (closed squares) #3 (open circles), #4 (closed circles), and #5 (closed triangles). As the fabrication process is refined, T_c increases and the transition width becomes narrower.

image was captured by using a cooled-CCD camera (Orca-ER, Hamamatsu).

3. Results

Figure 1(a) shows X-ray diffraction pattern of the final powder samples used for the wire #4 [18]. All peaks can be indexed by α-$ThCr_2Si_2$-type crystal structure, and no impurity peaks are identified. In the inset of Fig. 1(a), profiles of (116) diffraction peaks of powders used for the wire #2, #3, and #4 are compared. It is obvious that the new powder for wire #4 shows narrow peak profile and clear separation of $K_{\alpha 1}$ and $K_{\alpha 2}$ peaks is observed. This narrow diffraction peak also guarantees homogeneity of the grains in the wire core. In Fig. 1(b), the temperature dependence of magnetization is compared for the wire #2, #3, #4, and #5. As we successively introduced new processes for the improvement of wires, the onset of diamagnetism of the wire shifts to higher temperatures and the transition width becomes narrower. It should be noted that IBSs show strong sensitivity to strains, and T_c and volume fraction of superconductivity of the as-drawn wires are severely suppressed [17]. Only after proper sintering process, the value of T_c and volume fraction recover. In this sense, T_c as high as 36 K with very narrow transition width in the fabricated wire is not so obvious.

Figures 2(a), (b), (c), (d), (e) show optical micrographs of the cross section of the wires #1, #2, #3, #4, and #5, respectively. The corresponding MO images are shown in Fig. 2(f), (g), (h), (i), and (j), respectively. Obviously, the first generation wire #1 without HIP process shown in Fig. 2(f) is granular and low J_c is expected. Actually, transport J_c at 4.2 K and self-field for the wire #1 is only 1.0×10^4 A/cm^2 [15]. After introducing Ar-gas purification system, planetary ball milling, and high pressure sintering (HIP process) at 120 MPa, obvious granularity has been eliminated as shown in the image for wire #2 (Fig. 2(g)). Introduction of better-quality starting powders sustained the suppression of granularity as shown in Fig. 2(h). MO images keep to demonstrate large intergranular current after introducing refined powders by eliminating outer skin part of reacted materials in wire #4 (Fig. 2(i)). Now, the latest round wire partly drawn using dies has better geometrical symmetry of the core compared with earlier wires as shown in Fig. 2(j). One may notice some darker linear defects in some of MO images, as shown in upper half of Fig. 2(h). These are related to the cracks in the core of the wire which were introduced in the process of drawing. Similar crack formations have been reported in pressed tapes of 122-type IBSs [24]. The presence and direction of the cracks with respect to the current flow is responsible for the discrepancy between the J_c values evaluated by transport method and those evaluated magnetically [25].

Transport J_c as a function of magnetic field up to 140 kOe for wire #2 (open squares), #3 (closed

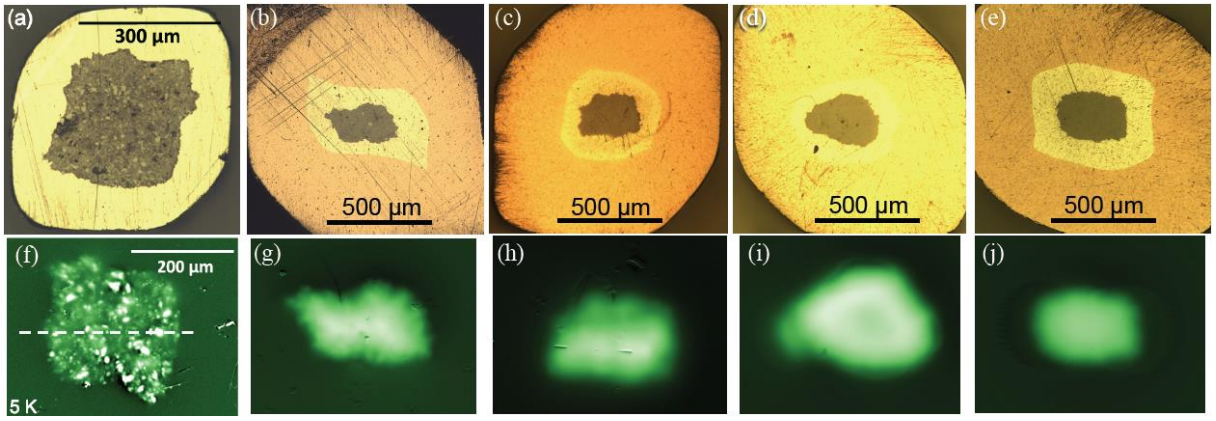

Figure 2. Optical micrographs of PIT wires (a) #1, (b) #2, (c) #3, (d) #4, and (e) #5. Corresponding MO images of PIT wires in the remanent state at 5 K (f) #1, (g) #2, (h) #3, (i) #4, and (j) #5.

squares), #4 (open circles), and #5 (closed circles) are shown in Fig. 3(a). It is obvious that transport J_c increases steadily as the fabrication process is refined. After the introduction of HIP process, the low-field J_c exceeded 1.0×10^5 A/cm^2, and it reached 2.0×10^5 A/cm^2 in wire #5. The transport J_c at 4.2 K under 100 kOe has also been enhanced steadily and reached 3.8×10^4 A/cm^2 in wire #5. In Fig. 3(b), transport J_c as a function of magnetic field for HIP tapes fabricated in parallel with HIP wires #4 (#4': open triangles) and #5 (#5': closed triangles) are shown in Fig. 3(b) [18]. It should be noted that HIP tape has better J_c characteristics compared with HIP wires especially at lower fields even if they are fabricated from the same starting powder.

4. Discussion

Let us discuss the reason why we obtained almost twice as large as J_c in wire #5 compared with wire #4 at high fields. Our initial intention of using wire-drawing dies was to make the shape of the core more symmetric and its density higher. However, it is well known that grains in the core of the PIT round wires of quasi-two-dimensional materials such as cuprate or MgB_2 are textured [26]. This is due to the plate-like shape of the grains. In order to confirm if grains in wire #5 are textured to some extent or not, we took X-ray diffraction pattern for two orthogonal cross sections shown in Figs. 4(e) and (f). In the case of X-ray diffraction from the longitudinal cross section (Fig. 4(c)), the intensity ratio of

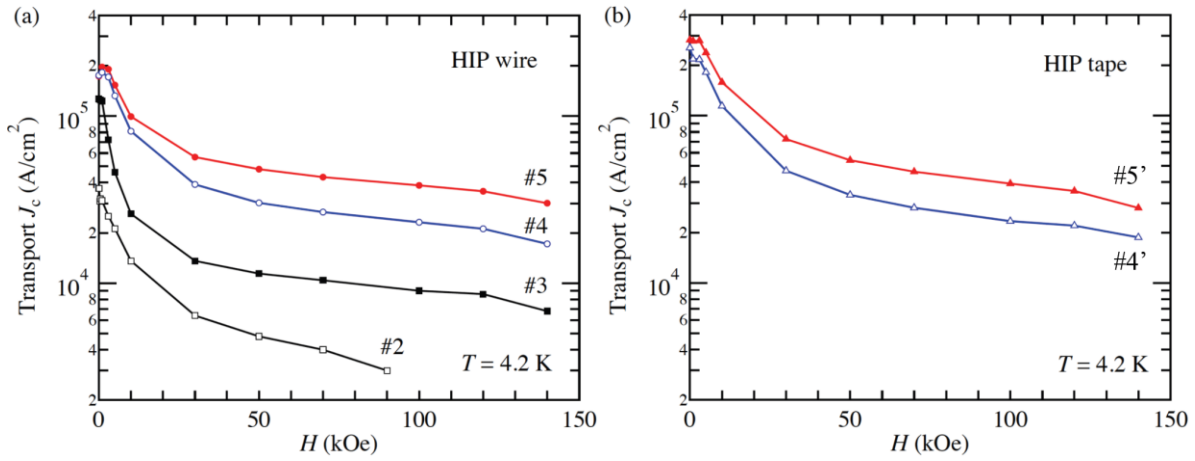

Figure 3. (a) Transport J_c as a function of field up to 140 kOe for wire #2 (open squares), #3 (closed squares), #4 (open circles), and #5 (closed circles). (b) Transport J_c as a function of magnetic field for HIP tapes fabricated in parallel with HIP wires #4 (#4': open triangles) and #5 (#5': closed triangles).

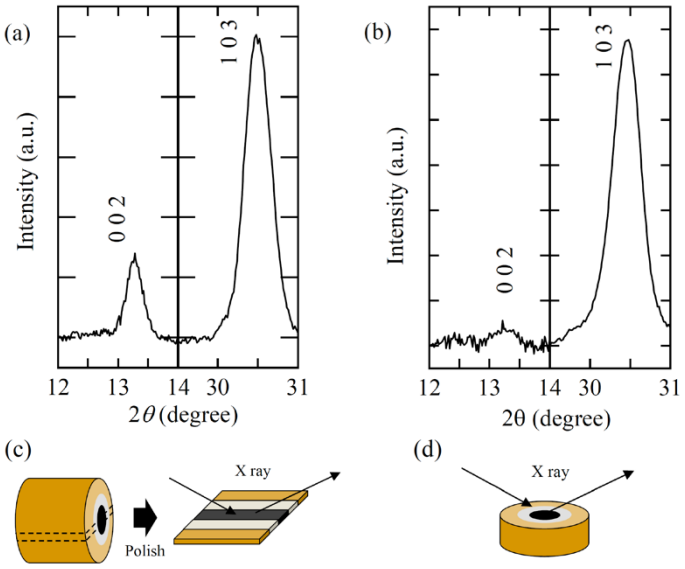

Figure 4. (a) X-ray diffraction profiles of (002) and (103) peaks taken for the longitudinal cross section shown in (c). The same taken for the transverse cross section shown in (d).

(002) and (103) peaks $I(002)/I(103) \sim 0.28$. On the other hand, in the case of transverse cross section (Fig. 4(d)), the same ratio $I(002)/I(103)$ is less than 0.06. The weaker $I(002)$ in the case of the transverse cross section indicates that the fraction of *c*-axis oriented grain on this surface is small. On the other hand, modest value of $I(002)/I(103)$ for the longitudinal cross section supports that fraction of *c*-axis oriented grains on this surface is not negligible. Such *c*-axis-oriented grains can couple along the direction of the wire and at least partly suppress weak-links. In the ideal case of round wires made out of quasi-two dimensional material with tetragonal symmetry, all grains are expected to align so that they become axisymmetric with respect to the center of the wire. To quantitatively evaluate the degree of texturing in the wire core, we may need to investigate the evolution of the X-ray diffraction intensity by successively exposing different surfaces at different depths or X-ray with much shorter wavelength may be necessary.

5. Summary

Present status of the development of round wires using 122-type iron-based superconductors is reviewed. Transport J_c has been enhanced by successive introductions of several techniques such as high-pressure sintering, control of drawing and sintering condition, promotion of the reaction of raw materials by densification, and introduction of dies in the drawing process, which enhanced the texturing inside the wire core. The present records of transport J_c of round wires are realized for that processed at 175 MPa with values at 4.2 K under self-field and 100 kOe being 2.0×10^5 A/cm^2 and 3.8×10^4 A/cm^2, respectively. HIP tapes processed in the same condition also demonstrated good performance with its transport J_c at self-field and 100 kOe being 2.8×10^5 A/cm^2 and 3.8×10^4 A/cm^2, respectively. We expect that further enhancement of J_c can be realized by enhancing the degree of texturing and further densification of the core using higher pressure.

6. References

[1] Ma Y 2012 *Supercond. Sci. Technol.* **25**, 113001
[2] Putti M *et al*. 2010 *Supercond. Sci. Technol*. **23**, 034003
[3] R Prozorov, Ni N, Tanatar M A, Kogan V G, Gordon R T, Martin C, Blomberg E C, Prommapan P, Yan J Q, Bud'ko S L and Canfield P C 2008 *Phys. Rev.* B **78**, 224506
[4] Nakajima Y, Taen T and Tamegai T 2009 *J. Phys. Soc. Jpn.* **78**, 023702

[5] Nakajima Y, Tsuchiya Y, Taen T, Tamegai T, Okayasu S and Sasase M 2009 *Phys. Rev.* B **80**, 012510
[6] Tamegai T, Taen T, Yagyuda H, Tsuchiya Y, Mohan S, Taniguchi T, Nakajima Y**,** Okayasu S, Sasase M, Kitamura H, Murakami T, Kambara T and Kanai Y 2012 *Supercond. Sci. Technol.* **25**, 084008
[7] Taen T, Nakajima Y, Tamegai T and Kitamura H 2012 *Phys. Rev.* B **86**, 094527
[8] Pyon S, Taen T, Ohtake F, Tsuchiya Y, Inoue H, Akiyama H, Kajitani H, Koizumi N, Okayasu S and Tamegai T 2013 *Appl. Phys. Express* **6**, 123101
[9] Ohtake F, Taen T, Pyon S, Tamegai T, Okayasu S, Kambara T and Kitamura H 2015 *Physica* C **518**, 47
[10] Taen T, Ohtake F, Pyon S, Tamegai T and Kitamura H 2015 *Supercond. Sci. Technol.* **28**, 085003
[11] Gao Z S, Wang L, Qi Y P, Wang D L, Zhang X P and Ma Y M 2008 *Supercond. Sci. Technol.* **21**, 105024
[12] Qi Y P, Wang L, Wang D L, Zhang Z Y, Gao Z S, Zhang X P and Ma Y W, *Supercond. Sci. Technol.* **23**, 055009
[13] Togano K, Matsumoto A and Kumakura H 2011 *Appl. Phys. Express* **4** 043101
[14] Weiss J D, Tarantini C, Jiang J, Kametani F, Polyanskii A A, Larbalestier D C and Hellstrom E E 2012 *Nat. Mater.* **11**, 682
[15] Ding Q P, Prombood T, Tsuchiya Y, Nakajima **Y** and Tamegai T 2012 *Supercond. Sci. Technol.* **25**, 035019
[16] Pyon S, Tsuchiya Y, Inoue H, Kajitani H, Koizumi N, Awaji S, Watanabe K and Tamegai T 2014 *Supercond. Sci. Technol.* **27**, 095002
[17] Pyon S, Yamasaki Y, Kajitani H, Koizumi N, Tsuchiya Y, Awaji S, Watanabe K and Tamegai T 2015 *Supercond. Sci. Technol.* **28**, 125014
[18] Pyon S, Suwa T, Park A, Kajitani H, Koizumi N, Tsuchiya Y, Awaji S, Watanabe K and Tamegai T 2016 *Supercond. Sci. Technol.* **29**, 115002
[19] Tamegai T, Pyon S, Ding Q P, Inoue H, Kobayashi H, Tsuchiya Y, Kajitani H and Koizumi N 2014 *J. Phys. Conf. Ser.* **507**, 022041
[20] Gao G S, Togano K, Matsumoto A and Kumakura H 2014 *Sci. Rep.* **4**, 4065
[21] Zhang X P, Yao C, Lin H, Cai Y, Chen Z, Li J Q, Dong C H, Zhang Q J, Wang D L, Ma Y W, Oguro H, Awaji S and Watanabe K 2014 *Appl. Phys. Lett.* **104**, 202601
[22] Adachi S, Murai Y, Tanabe K 2014 *Physica* C **483**, 67
[23] Inoue H, Tsuchiya Y, Tada S, Pyon S, Kajitani H, Koizumi N and Tamegai T 2014 *Physica* C **504**, 73
[24] Lin H, Yao C, Zhang X P, Zhang H T, Wang D L, Zhang Q J, Ma Y Wa, Awaji S and Watanabe K 2015 *Sci. Rep.* **4**, 4465
[25] Pyon S, Mine A, Suwa T and Tamegai T 2015 *Physica* C **530**, 76
[26] Bjoerstad R, Scheuerlein C, Rikel M O, Ballarino A, Bottura L, Jiang J, Matras M, Sugano M, Hudspeth J and Michiel M D 2015 *Supercond. Sci. Technol.* **28**, 062002

Acknowledgements
This work was partially supported by a Grant-in-Aid for Scientific Research (A) (17H01141), a Grant-in-Aid for Young Scientists (B) (16K17745), and the Japan-China Bilateral Joint Research Project by the Japan Society for the Promotion of Science (JSPS). We thank Z. Gao, K. Togano and H. Kumakura for valuable comments for the improvement of the quality of polycrystalline sample.